



Anti-bacterial Activity of Kalzhat Clay Functionalized with Ag and Cu Nanoparticles

Sana Kabdrakhmanova,^{1,*} K. S. Joshy,^{2,3} Aiswarya Sathian,³ Kadiran Aryp,^{1,4} Kydyrmolla Akatan,^{5,*} Esbol Shaimardan,⁴ Madiar Beisebekov,⁴ Temirkhanova Gulden,⁴ Ainur Kabdrakhmanova,^{1,4} Aida Maussumbayeva,⁶ Tomy Muringayil Joseph⁷ and Sabu Thomas^{3,*}

Abstract

The advent of multidrug-resistant microorganisms and associated outbreaks are major threats facing humanity. Therefore, additional approaches are being explored, so as to create new antimicrobial agents that can be utilized over multiple cycles. To this end, functionalized clay with metal nanoparticles for antimicrobial applications has been formulated. Natural Kalzhat clay from the Almaty region of Kazakhstan was functionalized with silver and copper nanoparticles, following their in-situ synthesis. The unprocessed Kalzhat clay was characterized using X-ray diffraction (XRD), scanning electron microscopy (SEM), Fourier-transform infrared spectroscopy (FT-IR), and elemental analysis (EDX). The clay was treated with sodium carbonate before functionalization. The EDX, FT-IR and XRD analysis of the clay confirmed the presence of bentonites. The synthesized nanoparticles of silver and copper were also characterized using transmission electron microscopy (TEM), FT-IR, and EDX analysis. TEM images of the nanoparticles confirmed a spherical morphology in the nano size range, with an average diameter of 29.85 ± 14.34 nm for AgNPs and of 75.37 ± 28.24 nm for CuNPs. The clay impregnated with Ag and Cu nanostructures showed excellent antimicrobial activity against pathogenic gram-positive (*Staphylococcus aureus*) and gram-negative (*Escherichia coli*) bacteria, with inhibition zones of 10.5mm (AgNP) and 25mm (CuNP), and of 8.5mm (AgNP) and 13.5mm (CuNP), respectively. Hence, such metal nanoparticles incorporated into clay show promising anti-bacterial application, suggesting that clay could be used as a functional material in order to limit the spread of bacteria in agricultural and biomedical applications.

Keywords: Nanoparticles; Clay; Anti-bacterial activity; Biomedical applications.

Received: 09 August 2023; Revised: 18 September 2023; Accepted: 19 September 2023.

Article type: Research article.

1. Introduction

Currently, there are many kinds of antibacterial agents available, which are very effective against pathogenic bacteria that can produce infection and disease. However, antibacterial resistance is constantly developing, which adversely impacts global health.^[1] Therefore, a lot of research has been carried out to develop new antibacterial agents with a broader range of effect. Clays have been used in many applications due to

their unique properties, high reactivity, and ease of adding functional components, which effectively enables clays to serve as smart materials with tunable properties. Clays have been well-researched in the past few decades, and continue to be a hot topic in the fields of agriculture and biomedicine.^[2] Antibacterial clays may offer an added environmentally benign complementary and alternative delivery vehicle when dealing with certain health problems. Further, such clays could act as an advantageous treatment option for certain skin infections, particularly in developing countries, which may have access to such common minerals, though lack proper health services in general. However, applying antibacterial clays safely and effectively, identifying how they affect pathogenic bacteria, and assessing potential resultant health issues need to be investigated.^[3,4]

A literature review showed that introduction of antibacterial compounds and ions of copper, silver and other metals into the matrix of natural clay created compounds that were effective against *Salmonella typhimurium* ATCC 14028,

¹ Department of Chemical and Biochemical Engineering, Satbayev University, Almaty, 050000, Kazakhstan.

² School of Nanoscience and Nanotechnology, Mahatma Gandhi University, Kottayam – 686 560, Kerala, India.

³ School of Energy Materials, Mahatma Gandhi University, Kottayam 686 560, Kerala, India.

⁴ Scientific Center of Composite Materials, Almaty, 050000, Kazakhstan

⁵ National scientific laboratory, S. Amanzholov East Kazakhstan University, Oskemen, 070020, Kazakhstan

Staphylococcus aureus ATCC 13565,^[5] *Bcc*, *Pseudomonas aeruginosa*, *Stenotropomonas maltophilia*,^[6] and *Staphylococcus epidermidis*. Further, such clay-based materials were shown to exhibit strong activity against the skin condition acne and related pathogens, including *Cutibacterium Acnes* and *Pseudomonas aeruginosa*.^[7]

The current study explores antibacterial functionalized Kalzhat clay, which is found in the Almaty region of Kazakhstan, and is mainly composed of bentonite. Kalzhat clay has been functionalized with antibacterial metals, specifically silver and copper. The metals have been anchored to the clay surface in order to form an inorganic antibacterial material, which is more favourable than organic counterparts in terms of safety, stability and functional longevity.^[8] The ion exchange properties of various clays play a significant role in functionalization. Silver and copper functionalized clay shows enhanced antibacterial properties due to the ability to exchange ions present in the clay with the added metal ions.^[9,10] The biocidal properties of silver ions have long been established, though the ability of any material to distribute them effectively and efficiently into clusters is key in achieving a desired outcome. Silver ions inhibit the proliferation of a number of bacteria, fungi and viruses,^[11-14] in a manner that exceeds many other materials or devices capable of limiting the spread of dangerous microorganisms. One can expand the use of the antibacterial properties of silver ions through functionalization with clay molecules. Yet, only a few studies have been done on elucidating the biocidal action of copper nanoparticles. The present research focuses on the development of copper and silver functionalized clay, so as to achieve a better understanding of the antibacterial properties of such a hybrid system. Of note is that the antibacterial action of hybrid nano systems is gaining tremendous importance in scientific circles.

In the present work, the bacteriostatic action of both silver and copper nanoparticles, inclusive of their functionalized clays, following examination of their antibacterial action on gram-positive and gram-negative bacteria, has been carefully evaluated. The results of the investigation are meant to expand the current knowledge of, as well as the potential application of, such antibacterial functionalized clays.^[15-17]

2. Materials and methods

2.1 Materials

Clay from the Kalzhat deposits (Almaty region, Kazakhstan) was sourced locally. Copper (II) sulfate pentahydrate, ascorbic acid, silver nitrate, sodium hydroxide, sodium citrate, and

glucose were purchased from Sigma Aldrich (India). All chemicals were used as is, without further purification. Further, all solutions were prepared using water filtered via the MilliQ Plus system (Merck, Germany).

2.2 Methods

2.2.1 Activation of Kalzhat clay (A- Kzh)

Modified Kalzhat clay (3g) was treated with sodium carbonate (Na_2CO_3 , 25 mL, or 2%), and stirred for about 1 hour, then 75 mL of water was added to raise the final volume to 100 mL. Stirring was continued for a further period of 2 hours, following which the solution was then filtered and air dried. The same procedure was repeated for different ratios of Na_2CO_3 (3%, 5% and 10%). After adding the required amount of Na_2CO_3 , the samples were heated to 70°C, and stirred for a 2 h, in order to ensure activation and improve the swelling process. At the end of this step, any water lost due to evaporation was replaced through the addition of deionized water, so as to maintain the same clay concentration in the suspension.^[18]

Depending on the concentration of Na_2CO_3 activated bentonites and the initial bentonite concentration, the compounds were designated: 2A-Kzh – Kalzhat clay with 2% Na_2CO_3 ; 3A-Kzh – with 3% Na_2CO_3 ; 5A-Kzh – with 5% Na_2CO_3 ; and, 10A-Kzh – with 10% Na_2CO_3 .

2.2.3 Synthesis of Ag nanoparticles (AgNPs)

The silver nanoparticles were prepared by dissolving silver nitrate (0.017%) in deionized water 100 mL, with a sodium citrate solution (0.03%) added to the resulting solution and stirred for 20 min in an ultrasonic bath. The solution was then stabilized using a glucose (1%) solution and kept in a water bath at 80°C for 30 min, until the formation of colloidal silver nanoparticles occurred. The synthesized nanoparticles were lyophilized and used for further characterization.^[18]

2.2.4 Synthesis of Cu nanoparticles (CuNPs)

Copper nanoparticles were synthesized using the chemical reduction method with a copper (II) sulfate pentahydrate precursor and starch as a capping agent. The precursor (0.1 M) was added to the starch (1.2%) solution, followed by 30 mins vigorous stirring. An ascorbic acid (0.2 M, 50 mL) solution was added to the resulting solution while rapidly stirring, followed by the addition of a sodium hydroxide (1M, 30 mL) solution. Stirring was continued at 80 °C for 2 hours, until the color of the solution changed from light yellow to dark yellow. The reaction was allowed to finish, then the solution was kept overnight under ambient conditions, after which the supernatant was discarded. The precipitates were separated by filtration, then washed with deionized water and ethanol, in order to remove any excess starch bound to the nanoparticles. After drying, the nanoparticles were stored in glass vials for characterization.^[19]

2.2.5 Functionalization of A-Kzh with silver nanoparticles

⁶ Department of *инженерия*, I. Zhansugurov Zhetysu University, Taldykorgan, 040009, Kazakhstan.

⁷ Department of Polymer Technology, Faculty of Chemistry, Gdańsk University of Technology, G. Narutowicza, 80-233 Gdańsk, Poland.

*Email: sanaly33@mail.ru (S. K. Kabdrakhmanova), ahnur.hj@mail.ru (K. Akatan), sabuthomas@mgu.ac.in (S. Thomas)

(A-Kzh/AgNPs)

The silver nitrate solution (0.017%) was added to a solution of sodium citrate (0.03%), then stirred for 20 min using a mechanical stirrer. A suspension of A-Kzh (0.5 g) was then added, followed by the addition of a glucose solution. The procedure was repeated for the preparation of Kalzhat clay with various concentrations of sodium carbonate. The silver functionalized clay was collected, washed, dried and used for further characterization.

2.2.6 Functionalization of A-Kzh with copper nanoparticles (A-Kzh/CuNPs)

0.1 M copper (II) sulfate pentahydrate solution was added into 120 mL of A-Kzh, followed by vigorous stirring for 30 min. The procedure was repeated for the preparation of Kalzhat clay with various concentrations of sodium carbonate. The copper functionalized clay was collected, washed and dried for further analysis.

3. Characterization

SEM analysis of Kzh clay and A-Kzh were performed using a JSM-6390 scanning electron microscope (JEOL, Japan). The TEM analysis of AgNPs, CuNPs and A-Kzh/AgNPs, A-Kzh/CuNPs were carried out using a JEM-2100 transmission electron microscope (JEOL, Japan) with an operating voltage 200 kV. The samples for TEM analysis were prepared by dispersing nanoparticles and functionalized clay powder in water and placing them onto a carbon-coated copper grid, followed by air drying. The FT-IR analysis of the AgNPs, CuNPs and A-Kzh/AgNPs, A-Kzh/CuNPs were performed using a Spotlight 400 FT-IR spectrometer (Perkin Elmer, USA) with a range of 400-4000 cm^{-1} . Structural features of the Kzh and A-Kzh, as well as A-Kzh/AgNPs and A-Kzh/CuNPs, were examined using a Miniflex 600 powder X-ray diffractometer (Rigaku, Japan), with an X-ray source of $\text{Cu } \alpha$ radiation ($\lambda = 1.54 \text{ \AA}$), an operating voltage of 40-kV, and an operating current of 15-mA. The X-ray diffraction patterns were recorded with the 2θ values, ranging between 10 and 80° , at a scan rate of 2° per min. EDX analysis of A-Kzh was performed utilizing a JEM 2100 transmission electron microscope (JEOL, Japan), with an operating voltage 200 kV.

3.1 Antimicrobial testing

The antimicrobial activity of A-Kzh/AgNPs and A-Kzh/CuNPs was tested against gram-positive *Staphylococcus aureus* and gram-negative *Escherichia coli* bacteria, utilizing the Kirby Bauer agar diffusion test. The bacterial strains were cultured in Mueller-Hinton broth at 37°C , for 12 h. Then 100 μL of each bacterial suspension was spread uniformly on nutrient agar. Discs of the AgNP and CuNP functionalized clay, as well as of the unprocessed clay, were cut into 6mm-diameter circular pieces and placed on the surface of the Mueller-Hinton Agar (MHA) plates. For comparison, a control disc. The culture plates were kept overnight at 37°C for incubation. The inhibition zones that developed were

measured in millimeters (mm). The experiment was repeated in triplicate, with results expressed as mean \pm SD.

4. Results and discussion

4.1 Morphology and qualitative chemical composition

The Kalzhat clay was functionalized with metal nanoparticles in order to study the antibacterial activity of the clay for future agricultural applications. Surface morphology of unprocessed Kzh and A-Kzh clay are shown in Fig. 1. The figure demonstrates that the surface morphology of Kalzhat clay was not uniform, as it contains different-sized grains of clay minerals. Because there were no significant changes in the surface morphology of the clay treated with various concentrations of sodium carbonate, in further studies the research team exclusively utilized the 2A-Kzh sample.

The particle distribution was not homogeneous, as the samples have different-sized grains, a characteristic of this group of clays.^[18] The varying lamellae properties and lack of defined particle sizes are indicative of the porousness of the clay. Figs. 1(c), (d), (e) and (f), shows a small increase in particle roughness caused by thermal treatment. The scanning electron micrograph (Fig. 1) of the bentonite clay indicates the presence of plate-like particles, as well as globular shaped ones, the latter of which are due to the presence of impurities (unfractionated components) in the clay.

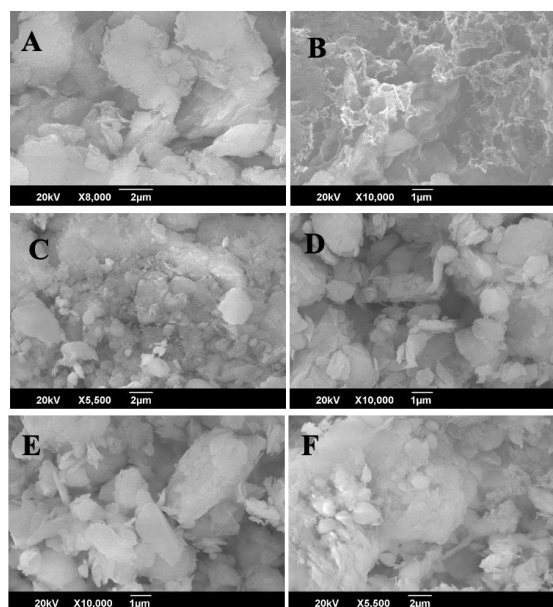


Fig. 1 SEM images of A, B) Kzh; C) 2A-Kzh; D) 3A-Kzh; E) 5A-Kzh; and, F) 10A-Kzh.

4.2 Analysis of Initial and metal functionalized clay

Qualitative chemical analysis of the bentonite Kalzhat clay is shown on Table 1. The most abundant components of these samples are Fe, Si and Al, which are the main components of clay. The presence of Ca, Mg, Fe, K, Ba and Ti are observed in the unprocessed Kalzhat bentonite.^[20] The presence of Ti in its oxide form occurs in small quantities without changing the properties of the clay.^[20] The content of Mg, Ca and K indicates the presence of exchangeable cations suitable for the

adsorption process. A comparative analysis of the elemental composition of the initial clay^[18] and samples following carbonate activation establish that the content of iron and cobalt decreases, while an increase in the amount of silicon, aluminum and calcium occurs. After activation with sodium carbonate, the presence of carbon and sodium was detected (Table 1). This in turn increases the exchange capacity of the clay, improving its adsorption property. Therefore, following this activation, the Kalzhat clay transitions to sodium montmorillonite mixed with a small amount of calcium montmorillonite. The cation exchange capacity of the original bentonite clay was low compared to commercially available synthetic montmorillonite.^[20,21]

Table 1. Elemental analysis of 2A- Kzh clay.

Element	Weight %	Atomic%
Fe	28.94	49.53
C	8.58	13.21
Na	2.55	2.05
Al	14.50	9.95
Si	33.79	22.26
Ca	0.31	0.14
B	1.11	0.37
Co	0.59	0.18
Cu	7.01	2.04
Hf	1.66	0.17
Au	0.96	0.09
Total	100.00	

4.3 FTIR spectroscopic structural analysis

Figure 2 shows the IR spectra of bentonite functionalized with copper and silver nanoparticles, as well as separate spectra for the metal nanoparticles themselves. The bentonite clay has the following characteristic bands: 3400–3700 cm^{-1} (OH stretching of Si-OH groups); 1640 cm^{-1} (deformation vibrations of the interlayer water in the clay); and, 1030 cm^{-1} (asymmetric Si-O-Si stretching). The band at 1014 cm^{-1} can be assigned to the Si-O bond in the Kalzhat clay. The FTIR spectrum in the hydroxyl region shows a peak at 3454 cm^{-1} , whereas that at 3409 cm^{-1} is for the silanol -OH group. Peaks at 1654 cm^{-1} and 1609 cm^{-1} were indicative of the O-H stretching vibrations in the clay. In this study, the FT-IR spectra of the bentonite-containing Kalzhat clay shows an absorption band at 3695.17 cm^{-1} , which is due to the stretching vibration of OH groups, and relates to alcohols and phenol-type compounds. The appearance of a band at 796.59 cm^{-1} seems due to AlAMgAOH stretching, confirming the presence of quartz, which was then confirmed by X-ray diffraction. Two weak bands at 938.81 cm^{-1} and 1421.46 cm^{-1} are caused by OAH bending of the carboxylic acid group and CAH bending of alkanes, respectively. The FTIR spectra for both the functionalized clay samples are almost the same, except for the presence of extra peaks at 2925 and 2854 cm^{-1} , due to the meth (Figs. 2a-2b). The disappearance of stretching and bending vibrations of Al_2eOH at 3620 and 915 cm^{-1} indicate

the broken Al_2eOH bonds. The broad band at 3200–3600 cm^{-1} is attributed to an -OH stretching vibration, whereas water molecules absorbed on showed an -OH bending vibration at 1638 cm^{-1} .^[22] The broad band around 1000 cm^{-1} was assigned to the stretching band of SiO and AlO. The small band at 450–500 cm^{-1} was assigned to the skeletal vibrations of SiOeAl.^[23]

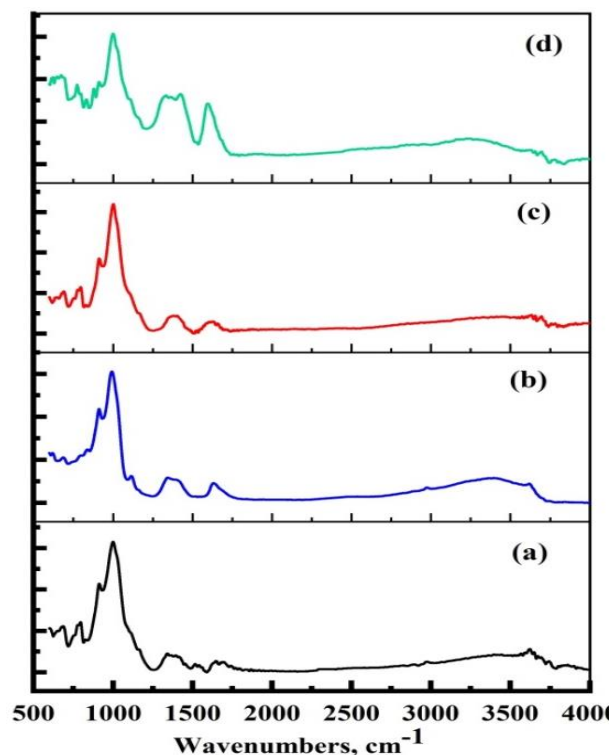


Fig. 2 FTIR spectra of a) A-Kzh/AgNPs; b) A-Kzh/CuNPs; c) AgNPs; and, d) CuNPs.

4.4 TEM analysis

The TEM micrographs of the A-Kzh/AgNPs, A-Kzh/CuNPs, AgNPs and CuNPs are shown in Fig. 3. TEM results demonstrate that silver and copper nanoparticles were successfully incorporated into the Kalzhat bentonite (Figs. 3A-3B). In the figures, the spherical morphology of both the silver and copper NPs are clearly seen to be present on the surface of the layered Kalzhat clay. This also confirms general uniform distribution of Ag and Cu nanoparticles on the clay surface, and indicates the absence of any major agglomeration of the nanoparticles on the layers of the clay. Compared to the size of the AgNPs alone, the average size was found to increase following addition to the clay. Nanoparticle size was determined utilizing Image J software. The size of AgNPs in the functionalized Kalzhat was 72.66±23.8 nm. In the case of the CuNPs, the average size was found to be 75±26.9 nm following addition to Kalzhat clay (Fig. 3B). TEM images show the morphology of the AgNPs and particles were around 29.85±4.34 nm in size. In Fig. 3C all the AgNPs are almost spherical in shape, with no aggregation seen. The glucose molecules seem to have successfully stabilized the nanoparticles and prevented their aggregation. The TEM

image in Fig. 3D shows that the copper nanoparticles were uniform in diameter with a range of 75.37 ± 28.24 nm, and had a somewhat polygonal shape. Larger particles with an increased size were also observed along with a few smaller particles. The smaller-sized NPs in solution were due to effective stabilization of the nanoparticles by starch in solution. Apparently, functionalized Kalzhat clay imparts additional stability to nanoparticles, preventing their agglomeration.

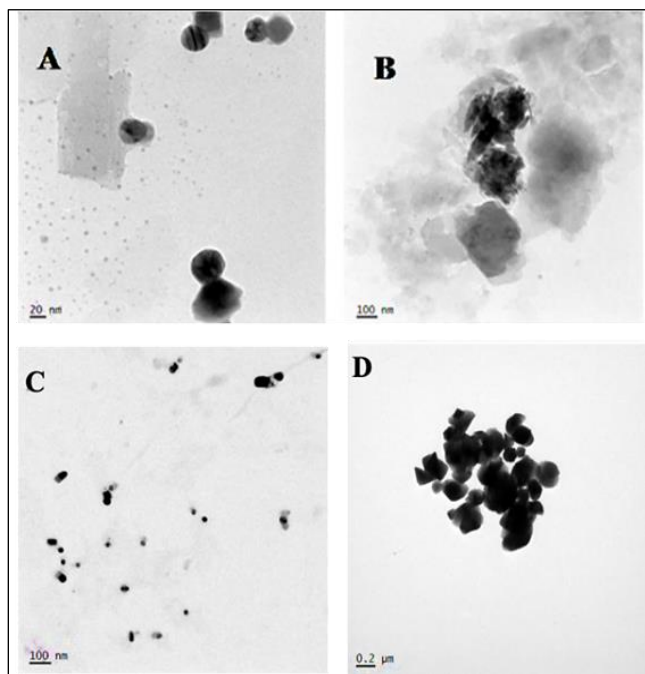


Fig. 3 TEM images of A) A-Kzh/AgNPs; B) A-Kzh/CuNPs; C) Ag Nps; and, D) CuNps.

4.5 Characterization of the clay and NPs using X-ray diffraction

Generally, the structural features of the materials were determined using XRD, allowing examination of any exfoliation or intercalation. The XRD analysis of unprocessed Kzh clay is shown in Fig. 4A, in which the peaks of bentonite can be clearly seen to start from $2\theta = 19.07$ and end at $2\theta = 49.67$, with particular peaks located at 2θ : 19.73, 20.99, 26.95, 34.87, 36.87, 39.57 and 50.12. The patterns identified contain silicon oxide (SiO_2), low quartz, low cristobalite, sodium ozonide and magnesium silicate. The XRD analysis of A-Kzh is shown in Fig. 4B, from which the peaks of bentonite are seen to range from $2\theta = 19.37$ to $2\theta = 50.03$, with specific peaks located at 2θ : 19.37, 20.63, 26.77, 34.87, 36.84, 39.81 and 50.03. The patterns identified contain silicon oxide (SiO_2), low quartz, low cristobalite, sodium ozonide and magnesium silicate. The XRD peaks of montmorillonite (8.8° and 19.7°) in bentonite almost disappeared. In addition, new X-ray diffraction peaks (26.5° and 35.5°) emerged and corresponding to quartz. The structural changes were due to dehydration, dihydroxylation processes, and formation of the crystalline structure during the calcination process.^[20,24] The appearance of strong and sharp diffraction peaks indicates that the synthesized bentonite-zeolite has been well crystallized.

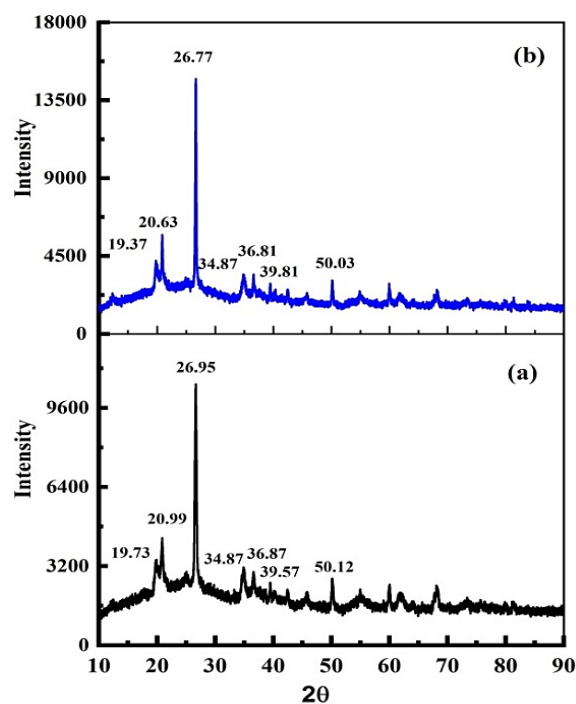


Fig. 4 XRD images of a) Kzh; and, b) A-Kzh.

The XRD pattern of AgNPs (Fig. 5c) shows a peak corresponding to the (200) plane,^[25] which resembles JCPDS card no.03-065-2871, and confirms the crystalline nature of the AgNPs. The structure of AgNPs is cubic, and the crystallite particle size was 0.408 nm, with an interplanar distance of 0.236 nm. Whereas, the XRD pattern of CuNPs (Fig. 5b) shows a peak corresponding to the (111)^[26,27] plane of face centered cubic (FCC) Cu crystals. The crystallite size of CuNPs was calculated using Scherrer's equation and found to be in the range of 5-40 nm.

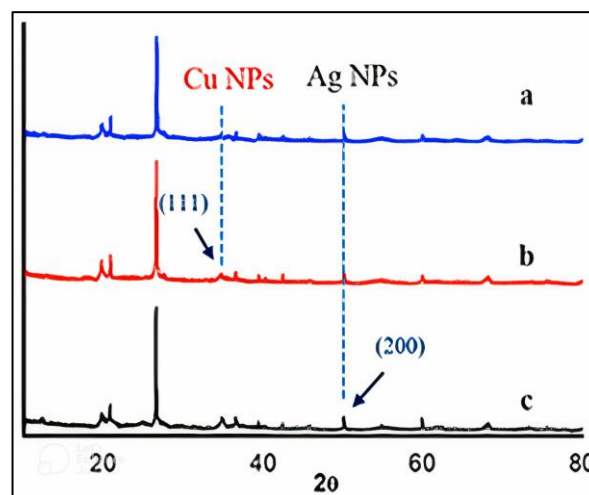


Fig. 5 XRD images of a) A-Kzh; b) CuNPs; and, c) AgNPs.

4.6 Antibacterial analysis

The antibacterial activity of the AgNP and CuNP functionalized Kalzhat clay samples was assessed by studying their inhibitory activity, utilizing the disc diffusion method, against human pathogens, gram-positive (*Staphylococcus*

aureus) and gram-negative (*Escherichia coli*) bacteria, the results of which are shown in Fig. 6. Clear inhibition zones of 10.5mm and 13.5mm diameters were observed around the discs placed in the *E. coli* and *S. aureus* samples, respectively, while no zone formation took place around the discs of unprocessed or activated Kalzhat clay. These results clearly reveal that the addition of metal nanoparticles provides a high antimicrobial activity to the Kalzhat clay. The mechanism behind the enhanced antibacterial activity appears to involve the adsorption of metal ions onto the surface of the clay, the generation of reactive oxygen species, and the impairment of the cell membranes of the bacteria. Due to the interaction of the metal ions with the thiol groups, alterations to proteins result in inactivation of enzymes and ultimately in protein leakage. The breakdown of proton motive force and disentanglement of respiratory reactions finally lead to bacterial death. Furthermore, due to the small size and high surface area provided by the nanoparticles, they successfully attach to the bacterial membranes, which also enhances the likelihood of bacterial death. Therefore, the size, shape and environmental conditions of the metal nanoparticles positively influence their antibacterial properties. In this study, the addition of metal nanoparticles to Kalzhat clay prevents the agglomeration of the nanoparticles through efficient immobilization on the surface of the clay, without using any further requisites, thus improving their effective antimicrobial property. As well, the inhibition zone in the *S. aureus* sample was observed to be more than that in the *E. coli* sample, which apparently demonstrates that the nanoparticles efficiently damage the thicker peptidoglycan cell layers of gram-positive bacteria more than the thinner peptidoglycan cell wall of the gram-negative bacteria. Finally, this simple and cost-effective method of adding metal nanoparticles to activated Kalzhat clay offers several promising applications, including products for the biomedical, cosmetics and agricultural sectors.

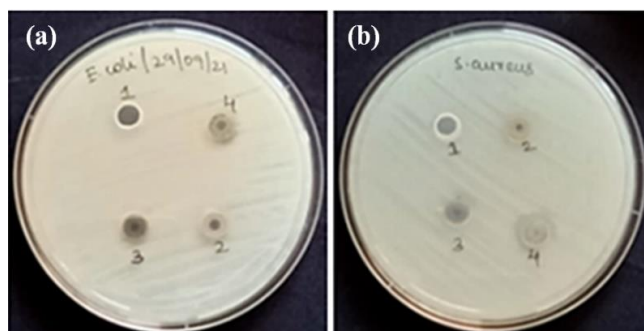


Fig. 6 The antimicrobial activity of different clay samples against a) *Escherichia coli*, with 1) control, 2) A-Kzh, 3) A-Kzh/Ag NPs, and 4) A-Kzh/Cu NPs; b) *Staphylococcus aureus*, with 1) control, 2) A-Kzh, 3) A-Kzh/Ag NPs, and 4) A-Kzh/Cu NPs.

5. Conclusion

In the present study, infusion of silver and copper nanoparticles into activated Kalzhat clay was successfully investigated following characterization using SEM-EDX, TEM and XRD, which confirmed the presence of

nanoparticles on the clay surface. Antibacterial studies were carried out, with the results showing that the synthesized AgNP and CuNP functionalized clay exhibited good antimicrobial activity against human pathogenic bacteria, including *Escherichia coli* (gram-negative) and *Staphylococcus aureus* (gram-positive), with inhibition zones of 30 mm (AgNP) and 26 mm (CuNP), and of 30 mm (AgNP) and 26 mm (CuNP), respectively. The authors recommend the application of such functionalized Kalzhat clay in the agricultural sector, in order to control the spread of disease between seed stocks and between plants, perhaps as an additive to existing treatments, so as to limit the amount of potentially hazardous agrochemicals utilized. Further, as mentioned in the text, application in biomedicine as a topical solution in underdeveloped economies may also be a strong option.

Acknowledgments

This work was supported by the Science Committee of the Ministry of Science and Higher Education of the Republic of Kazakhstan, Grant No. AP09260644. We are grateful to: Mahatma Gandhi University (India, Kerala) for providing the opportunity to conduct our research, to Sabu Thomas for supporting us, to Kantay Nurgamit, Paul Jacob and Kaiyrbekov Nariman for assistance during the experiment.

Conflict of Interest

There is no conflict of interest.

Supporting Information

Not applicable.

References

- [1] F. Bergaya, G. Lagaly, Chapter 1 general introduction: clays, clay minerals, and clay science. *Developments in Clay Science*. Amsterdam: Elsevier, 2006: 1-18, doi: 10.1016/s1572-4352(05)01001-9.
- [2] H. H. Murray, Overview—clay mineral applications, *Applied Clay Science*, 1991, **5**, 379-395, doi: 10.1016/0169-1317(91)90014-Z.
- [3] J.M. Amigo, J. Bastida, A. Sanz, M. Signes, J. Serrano, Crystallinity of Lower Cretaceous kaolinites of Teruel (Spain), *Applied Clay Science*, 1994, **9**, 51-69, doi: 10.1016/0169-1317(94)90014-0.
- [4] M. I. Carretero, Clay minerals and their beneficial effects upon human health. A review, *Applied Clay Science*, 2002, **21**, 155-163, doi: 10.1016/S0169-1317(01)00085-0.
- [5] N. N. Azmi, N. A. Mahyudin, W. H. Wan Omar, N.-K. Mahmud Ab Rashid, C. F. Ishak, A. H. Abdullah, G. J. Sharples, Antibacterial activity of clay soils against food-borne salmonella typhimurium and staphylococcus aureus, *Molecules*, 2021, **27**, 1-15, doi: 10.3390/molecules27010170.
- [6] S. Behroozian, J. E. A. Zlosnik, W. Xu, L. Y. Li, J. E. Davies, Antibacterial activity of a natural clay mineral against burkholderia cepacia complex and other bacterial pathogens

- isolated from people with cystic fibrosis, *Microorganisms*, 2023, **11**, 150-159, doi: 10.3390/microorganisms11010150.
- [7] A. R. Hamilton, M. Roberts, G. A. Hutcheon, E. E. Gaskell, Formulation and antibacterial properties of clay mineral-tetracycline and-doxycycline composites, *Applied Clay Science*, 2019, **179**, 105148, doi: 10.1016/j.clay.2019.105148.
- [8] G. S. Martynková, M. Valášková, Antimicrobial nanocomposites based on natural modified materials: a review of carbons and clays, *Journal of Nanoscience and Nanotechnology*, 2014, **14**, 673-693, doi: 10.1166/jnn.2014.8903.
- [9] M. Ghorbanpour, M. Mazloumi, A. Nouri, S. Iotfiman, Silver-doped Nanoclay with Antibacterial Activity, *Journal of Ultrafine Grained and Nanostructured Materials*, 2017, **50**, 124-131, doi: 10.22059/JUFGNSM.2017.02.07
- [10] A. Stavitskaya, S. Batasheva, V. Vinokurov, G. Fakhrullina, V. Sangarov, Y. Lvov, R. Fakhrullin, Antimicrobial applications of clay nanotube-based composites, *Nanomaterials*, 2019, **9**, 708-718, doi: 10.3390/nano9050708.
- [11] E. E. Gaskell, A. R. Hamilton, Antimicrobial clay-based materials for wound care, *Future Medicinal Chemistry*, 2014, **6**, 641-655, doi: 10.4155/fmc.14.17.
- [12] S.-I. Hong, J.-W. Rhim, Antimicrobial activity of organically modified nano-clays, *Journal of Nanoscience and Nanotechnology*, 2008, **8**, 5818-5824, doi: 10.1166/jnn.2008.248.
- [13] M.K. Uddin, A review on the adsorption of heavy metals by clay minerals, with special focus on the past decade, *Chemical Engineering Journal*, 2017, **308**, 438-462, doi: 10.1016/j.cej.2016.09.029.
- [14] R. S. Costa, E. A. B. Moura, A bibliometric analysis of the strategy and performance measurement of the polymer matrix nanomaterials development scenario globally, and the participation of Brazil. The Minerals, Metals & Materials Series. Cham: Springer International Publishing, 2020: 329-342, doi: 10.1007/978-3-030-36628-5_31.
- [15] T. M. Joseph, D. Kar Mahapatra, A. Esmaeili, Ł. Piszczyk, M. S. Hasanin, M. Kattali, J. Haponiuk, S. Thomas, Nanoparticles: taking a unique position in medicine, *Nanomaterials*, 2023, **13**, 574, doi: 10.3390/nano13030574.
- [16] S. Kesavan Pillai, S. Sinha Ray, M. Scriba, J. Bandyopadhyay, M. P. Roux-van der Merwe, J. Badenhorst, Microwave assisted green synthesis and characterization of silver/montmorillonite heterostructures with improved antimicrobial properties, *Applied Clay Science*, 2013, **83**, 315-321, doi: 10.1016/j.clay.2013.08.014.
- [17] M. Hariram, S. Vivekanandhan, Phytochemical process for the functionalization of materials with metal nanoparticles: current trends and future perspectives, *ChemistrySelect*, 2018, **3**, 13561-13585, doi: 10.1002/slct.201802748.
- [18] R. Md Akhir, S. Z. Umbaidillah, N. A. Abdullah, S. A. H. Alrokayan, H. A. Khan, T. Soga, M. Rusop, Z. Khusaimi, The potential of pandanus amaryllifolius leaves extract in fabrication of dense and uniform ZnO microrods, *Micromachines*, 2020, **11**, 299-310, doi: 10.3390/mi11030299.
- [19] A. Aradmehr, V. Javanbakht, A novel biofilm based on lignocellulosic compounds and chitosan modified with silver nanoparticles with multifunctional properties: synthesis and characterization, *Colloids and Surfaces A: Physicochemical and Engineering Aspects*, 2020, **600**, 124952, doi: 10.1016/j.colsurfa.2020.124952.
- [20] S. Kabdrakhmanova, K. Aryp, E. Shaimardan, E. Kanat, B. Selenova, K. Nurgamit, A. Kerimkulova, A. Amitova, A. Maussumbayeva, Acid modification of clays from the Kalzhat, Orta Tentek deposits and study their physical-chemical properties, *Materials Today: Proceedings*, 2023, **5**, 1-6, doi: 10.1016/j.matpr.2023.04.427.
- [21] M. I. Magzoub, M. S. Nasser, I. A. Hussein, A. Benamor, S. A. Onaizi, A. S. Sultan, M. A. Mahmoud, Effects of sodium carbonate addition, heat and agitation on swelling and rheological behavior of Ca-bentonite colloidal dispersions, *Applied Clay Science*, 2017, **147**, 176-183, doi: 10.1016/j.clay.2017.07.032.
- [22] A. Khan, A. Rashid, R. Younas, R. Chong, A chemical reduction approach to the synthesis of copper nanoparticles, *International Nano Letters*, 2016, **6**, 21-26, doi: 10.1007/s40089-015-0163-6.
- [23] O. Y. Golubeva, E. Y. Brazovskaya, Y. A. Alikina, Effect of acid activation on the sorption properties of synthetic montmorillonite, *Glass Physics and Chemistry*, 2022, **48**, 673-675, doi: 10.1134/s1087659622600466.
- [24] K. Tohdee, L. Kaewsichan, Asadullah, Enhancement of adsorption efficiency of heavy metal Cu(II) and Zn(II) onto cationic surfactant modified bentonite, *Journal of Environmental Chemical Engineering*, 2018, **12**, 2821-2828, doi: 10.1016/j.jece.2018.04.030.
- [25] M. M. Beisebekov, S. B. Serikpayeva, S. N. Zhumagalieva, M. K. Beisebekov, Z. A. Abilov, S. Kosmella, J. Koetz, Interactions of bentonite clay in composite gels of non-ionic polymers with cationic surfactants and heavy metal ions, *Colloid and Polymer Science*, 2015, **293**, 633-639, doi: 10.1007/s00396-014-3463-x.
- [26] L. F. Sukhodub, A. D. Pogrebnyak, L. B. Sukhodub, A. Sagidugumar, A. S. Kistaubayeva, I. S. Savitskaya, A. Talipova, A. Sadibekov, N. Kantay, K. Akatan, A. Turlybekuly, Antibacterial and physical characteristics of silver-loaded hydroxyapatite/alginate composites, *Functional Composites and Structures*, 2021, **3**, 045010, doi: 10.1088/2631-6331/ac3afb.
- [27] S. Kabdrakhmanova, E. Shaimardan, K. Akatan, B. Selenova, A. Zhilkashinova, D. Erbolatuly, M. Skakov, Preparation and characterization of the catalyst based on the copper nanoparticles, *International Journal of Nanoscience and Nanotechnology*, 2022, **18**, 1-10.

Publisher's Note: Engineered Science Publisher remains neutral with regard to jurisdictional claims in published maps and institutional affiliations.